

Inverter Based Distributed Generator Islanding Detection Method using Under/Over Voltage Relay

E. Kamyab* and J. Sadeh*

Abstract: Islanded operation of distributed generators is a problem that can happen when they are connected to a distribution system. In this paper an islanding detection method is presented for inverter based Distributed Generation (DG) using under/over voltage relay. The method is an adaptive one and is based on the change of DG active power reference (P_{ref}) in inverter control interface. The active power reference has a fixed value in normal condition, if the Point of Common Coupling (PCC) voltage changes, P_{ref} , is determined as a linear function of voltage. The slope of P_{ref} depends on the load active power (P_{load}) and it should be changed if P_{load} changes. The Non-Detection Zone (NDZ) of the proposed method is zero. If changing of the PCC voltage is sensed, islanding will be detected when it occurs. Also, it does not have any negative effects on the distribution system under normal conditions. The proposed method is evaluated according to the requirements of the IEEE 1547 and UL 1741 standards, using PSCAD/EMTDC software.

Keywords: Adaptive islanding detection, Inverter based distributed generation, Non detection zone, Under/Over voltage relay.

1 Introduction

Electric generation facilities which are connected to the power system through a Point of Common Coupling (PCC) in the load site are called Distributed Generation (DG) [1]. In this situation, one of the inevitable events is the islanding phenomenon, which happens when the local load is fed by the DG and the grid system has been interrupted. When the DG feeds the load independently in absence of distribution system the reliability and power quality would be aggravated. Moreover, it may threaten the safety of operational personnel who are repairing the distribution equipments. Therefore, the fast detection of islanding phenomenon is very important [2]. There are two types of islanding detection methods, local and remote techniques. While local techniques rely on the information and data of DG site, remote techniques are based on the communication between utility and the DG.

Supervisory Control And Data Acquisition (SCADA) [3] and power line signaling scheme [4-6] are used in remote techniques. Although, these techniques are more reliable than local techniques, they are more expensive than them to be implemented especially for small DGs [7].

Local methods are divided into passive, active and hybrids methods. For the methods that detect islanding

phenomenon passively, the upper and lower thresholds of a parameter of the power system should be defined in the DG site. If the parameter passes the threshold settings, the islanding is detected. The main advantages of passive methods are simplicity and inexpensiveness. These methods do not perturb the parameter of the system and have high accuracy when there is a large mismatch between generation and demand in the islanded system. Unfortunately, they have a serious problem of having relatively large Non Detection Zone (NDZ) and they may not be reliable in all loading conditions [8].

Active islanding detection techniques are utilized for increasing the reliability and reducing the NDZ. However, their use has some drawbacks which are shortly reported hereafter.

These methods introduce a small perturbation into the system. This small perturbation will make a severe change in system parameters in the absence of grid, whereas the change is insignificant when the DG is connected to the grid. Active methods are capable of detecting the islanding situation even if the DG generation matches the local load. Although active methods have a small NDZ, they can degrade the system power quality [9]. Moreover, the need for designing an additional controller in some active methods increases their complexity [10]. These methods can also cause problems under abnormal or transient grid conditions and can interfere among themselves in case of multiple generators.

Iranian Journal of Electrical & Electronic Engineering, 2012.

Paper first received 4 Sep. 2012 and in revised form 4 Nov. 2012.

* The Authors are with the Department of Electrical Engineering, Ferdowsi University of Mashhad, Mashhad, Iran.

E-mails: eb_ka635@stu-mail.um.ac.ir, sadeh@um.ac.ir.

Hybrid islanding detection techniques are a combination of active and passive methods. In these methods, the active technique is applied when islanding is undetectable by the passive method.

In [8], an active islanding detection method is presented for inverter based DG which drifts the PCC voltage to detect the islanding phenomenon. Based on the results of their study (Table I of [8]), it was pointed out that the NDZ of their presented method, is small but not zero. In [11], in order to detect the islanding phenomenon, a voltage positive feedback is designed in the synchronous d-q frame. It can be implemented on the inverter based DG and the method is based on the voltage drifting. However, the PCC voltage was unstable due to positive feedback in islanding condition.

Several active methods like Active Frequency Drift (AFD), Active Frequency Drift with Positive Feedback (AFDPF) [12] and slip mode frequency shift (SMS) [13] are presented and developed. In AFD method, for islanding detection, the current is slightly disturbed presenting a zero-current segment. So, it degrades the system power quality. AFDPF is an improved AFD method with positive feedback which has a very small NDZ; however, the converter output current is always discontinuous with AFDPF technique [12]. Slip mode frequency shift is similar to AFD except that the starting angle of the DG output current varies with frequency at each zero crossing of the terminal voltage. This method uses positive feedback to destabilize the inverter based DG in islanding condition [13]. SMS method has a small NDZ; however, output power quality of the DG and the power quality in a system with high DG penetration are decreased [9]. Some other islanding detection methods are reviewed in [9, 14, 15].

In order to overcome the shortcomings posed by active and passive methods, in the present study, an adaptive islanding detection method is presented with zero NDZ which only uses Under/Over (U/O) voltage relays. The DG is designed to operate in unity power factor and the local load is modeled as a voltage and frequency dependent load. The proposed technique has been applied in inverter based distributed generation and relies on the change of P_{ref} of DG in inverter control interface. In normal conditions, P_{ref} has a fixed value; however, when the voltage changes, it is determined as a linear function of voltage. The slope of P_{ref} depends on the load active power (P_{load}). The proposed method does not enter any perturbation into the system; hence it does not have any harmful effects on the distribution system and is relatively fast in islanding detection.

2 Power System, DG and Load Modeling

Fig. 1 shows the case study system which consists of a simple three-phase network with a grid connected DG system and a local load.

The DG is inverter based and connected to a 380V system through a 100 kVA transformer. The grid system is modeled by a 20 kV line to line voltage source with

125 MVA Short Circuit Capacity (SCC), which is connected to a 380V system using a 20 kV/0.380 kV, 100 kVA transformer and a 380V distribution line. The system parameters are presented in the Appendix.

Constant power control and constant current control are two mainly used control schemes in DG system. In the DG system which employs constant power control scheme, the active and reactive powers are controlled as constant. In the DG system which employs constant current control scheme, the current injected into the grid is controlled as constant. In this paper, distributed generation is modeled as a constant power with an interface control as proposed in [16]. The DG operates at unity power factor. The DG interface control variables are controlled in the d-q axis synchronous reference frame. Variables of d-q axis and DG interface control are used to calculate the modulation index and phase angle.

The load active and reactive power as function of voltage and frequency are expressed as follows [17]:

$$P = P_0 \left(\frac{V}{V_0} \right)^p (1 + k_p \Delta f) \quad (1)$$

$$Q = Q_0 \left(\frac{V}{V_0} \right)^q (1 + k_q \Delta f) \quad (2)$$

where V_0 represents the system nominal voltage, p and q are the voltage exponents of load active and reactive powers, k_p and k_q are frequency dependency factors of active and reactive powers, Δf is frequency deviation in per-unit and P_0 and Q_0 represent the load active and reactive powers corresponding to the nominal voltage. The exponents p and q vary between 0 and 2 and, k_p and k_q can change from 0 to 3 and -0.2 to 0, respectively [17].

3 Proposed Islanding Detection Method

In abnormal condition when the PCC voltage is in a range given in Table 1, the DG should be stopped to energize the power system within the clearing time as indicated in [18]. Clearing time is the time between the start of the abnormal condition and the DG ceasing to energize the power system. The purpose of the allowed

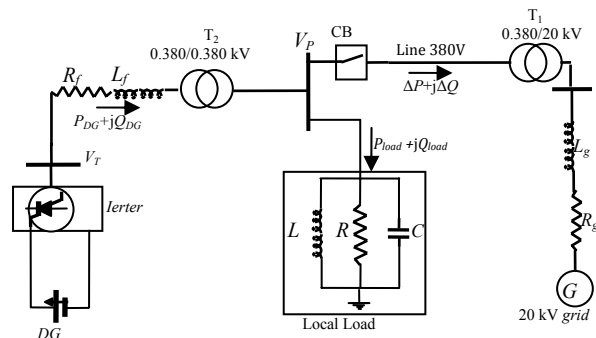


Fig. 1 Grid connected DG system with local load.

Table 1 Response to abnormal voltages [9, 18, 20].

Voltage (at PCC)	Maximum trip time
V < 50%	6 cycles
50% < V < 88%	120 cycles
88% < V < 110%	Normal operation
110% < V < 137%	120 cycles
V > 137%	6 cycles

time delay is to ride through short-term disturbances to avoid excessive nuisance tripping [18]. Also, low voltage ride through (LVRT) algorithm is considered for DG unit to avoid low voltage tripping due to temporary short circuit or dip voltage [19].

In order to detect the islanding by U/O voltage relay, post-islanding PCC voltage should be decreased/increased less/greater than 0.88/1.1 of nominal voltage [20, 21]. In Fig. 1, if the active power exchange between the DG and grid system before islanding (ΔP) is small, the PCC voltage remains in the above mentioned limits and islanding cannot be detected.

As mentioned in the authentic references [9, 18, 20] loads with $p=2$ (parallel RLC) are the worst case for islanding detection. Therefore, the method is formulated for parallel RLC load.

The following equations can be used for determining the NDZ considering before and after islanding PCC voltages.

$$P_{l0} = P_{lBI} = P_{DG} - \Delta P = \frac{V_p^2}{R} = \frac{(V_0 + \Delta V)^2}{R} \quad (3)$$

$$P_{lAI} = P_{DG} = \frac{V_p^2}{R} \quad (4)$$

where, V_p and V'_p are pre-and post-islanding PCC voltages, respectively. Also, $P_{lBI} = P_{l0}$, P_{lAI} , P_{DG} , ΔP and R are pre- and post-islanding load active power, DG active power generation, active power exchange between DG and grid system and local load resistance, respectively. In Eq. (3) V_0 is the grid nominal voltage in the 380 V transformer side and ΔV can be calculated as $\Delta V = \Delta I Z_0$, where Z_0 is the Thevenin impedance of grid seen from 380V transformer side. If reactive power of DG is equal to zero and load power factor is almost 1, then ΔV can be written as follows:

$$\Delta V \approx \frac{\Delta P Z_0}{V_0} \quad (5)$$

Substituting Eq. (5) into Eq. (3) and removing R between Eq. (3) and Eq. (4) and some manipulations, Eq. (6) can be written:

$$1 - \frac{\Delta P}{P_{DG}} = \frac{(1 + \frac{\Delta P Z_0}{V_0})^2}{(\frac{V'_p}{V_0})^2} \quad (6)$$

Using Eq. (3) and Eq. (4), the load active power can be calculated as Eq. (7).

$$P_{lAI} = P_{DG} = \frac{V_p^2}{V_0^2} P_0 \quad \text{or} \quad P_{DG} = \frac{V_p^2}{V_0^2} P_{l0} \quad (7)$$

Also, from Eq. (6), if $Z_0=0$ (grid is considered as infinity bus) the active power exchange between DG and grid can be calculated as follows:

$$\Delta P = P_{DG} (1 - \frac{V_0^2}{V_p^2}) \quad (8)$$

The NDZ can be obtained by substituting upper and lower bounds of voltage ($V_p/V_0=1.1$ and 0.88) into Eq. (6); that results in the following inequality when $Z_0=0$ [8, 10]:

$$- \%29.132 < \frac{\Delta P}{P_{DG}} < \%17.355 \quad (9)$$

It is important to note that, Eq. (9) is correct if the short circuit capacity of grid is assumed to be infinity and $V_0=380$ V, otherwise, NDZ should be calculated from Eq. (6). If active power exchange between the DG and the grid is in the non-detection zone, the islanding phenomenon cannot be detected. To detect the islanding phenomenon, P_{ref} is determined adaptively based on the values of DG generation and active power of local load. It is worth noting that the worst case of islanding detection happens when the power mismatch between the load active power and DG generation is almost zero. In such condition, there is no power exchange between the DG and the grid in nominal voltage. In order to clarify the subject, suppose $P_l = P_0 = P_{DG}$ ($\Delta P=0$) in nominal voltage V_0 . Besides, suppose that the system voltage changes to V_1 due to non-islanding phenomena. Then, $P_l = P_0 (V_1/V_0)^2$ and $\Delta P = P_{DG} (1 - V_1^2/V_0^2)$. In such condition, if islanding occurs, the PCC voltage changes from V_1 to V_0 after islanding. On the other hand, by the conventional islanding detection method, islanding detection is not possible. But as the pre- and the post-islanding PCC voltage are not equal, it is possible that the islanding phenomenon occurs. Using the proposed method, the islanding will be detected even in such cases. In other words, the PCC voltage variation is sensed by the voltage measurement and P_{ref} switches from P_{ref0} to a new P_{ref} and as a result, the proposed method drifts the voltage deviation to settle out the above mentioned limits, i.e. islanding is detectable.

To explain the proposed method more precisely, refer to Fig. 2. In this figure, the load active power characteristic and DG active power reference are drawn in respect to $r_{iv0} = V_p'/V_0$. The curves C_1 , C_2 , C_3 and C_4 are loads with $P_0 = P_{ref0}$, $P_0 = 1.03 P_{ref0}$, $P_0 = 1.1 P_{ref0}$ and $P_0 = 0.95 P_{ref0}$, respectively.

By measuring the post-islanding PCC voltage and voltage deviation from nominal voltage, the curve of the load active power in normal condition (P_0) can be determined. For instance, as shown in Fig. 2, if the voltage deviation is equal to $\Delta V_1 > 0$, then, the load active power curve is matched with curve C_4 . In this

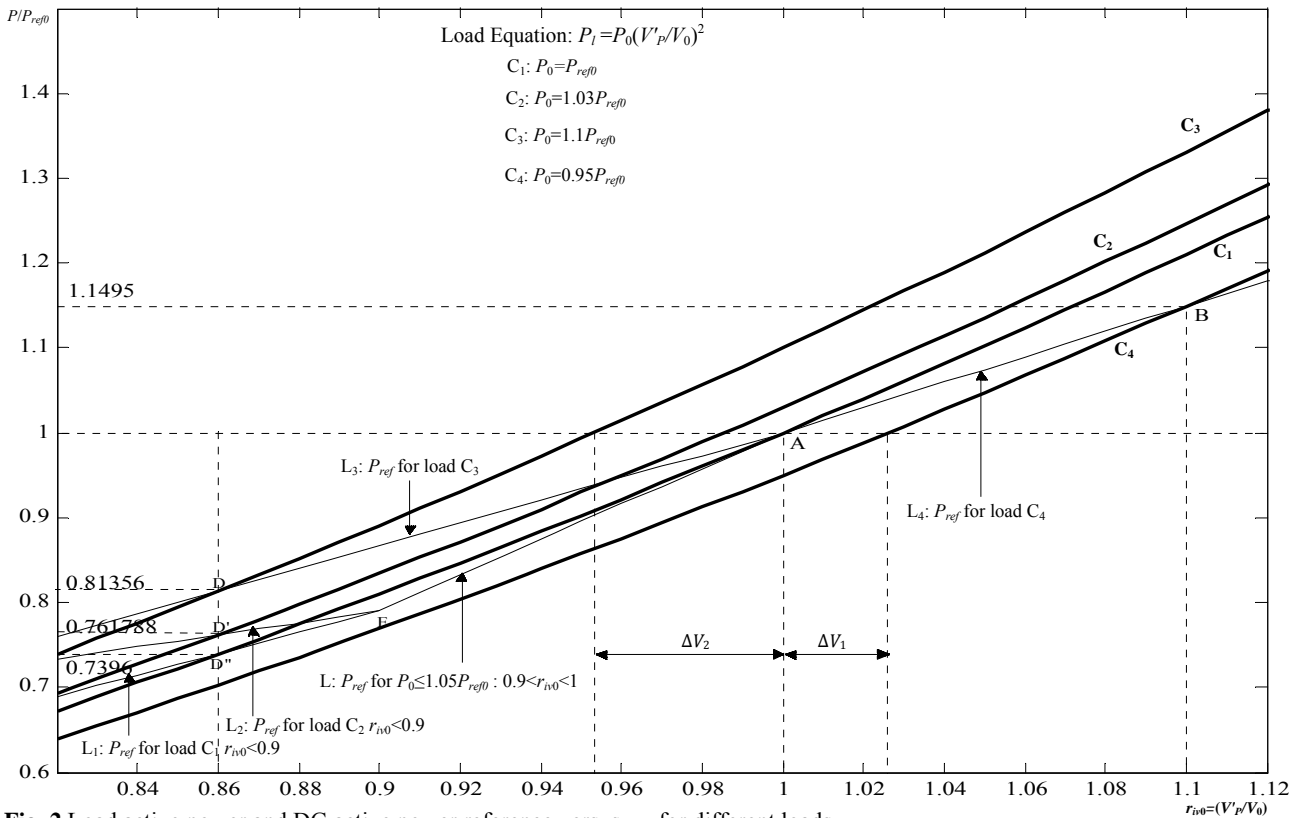


Fig. 2 Load active power and DG active power reference versus r_{iv0} for different loads.

condition, P_{ref} is determined as a linear function of voltage that passes through point A(1, P_{ref0}) and a point like B. The r_{iv0} of point B should be equal or greater than 1.1. Therefore, the PCC voltage is deviated to point B in islanding condition. Since the islanding voltage ratio of this point is equal or greater than 1.1, the islanding phenomenon will be detected. If r_{iv0} of point B is assumed to be 1.1, i.e. B(1.1, $1.21P_0$), the P_{ref} is determined as Eq. (10) for $\Delta V > 0$.

If the voltage deviation is $\Delta V_2 < 0$, then, the curve of the load active power is fitted to the curve C_3 with $P_0 = 1.1P_{ref0}$, as shown in Fig. 2. In this condition, P_{ref} is determined as a linear function of voltage that passes through points A(1, P_{ref0}) and a point like D. The r_{iv0} of point D should be equal or less than 0.88. Therefore, the PCC voltage is deviated to point D in islanding condition. Since the islanding voltage ratio of this point is equal or less than 0.88, the islanding will be detected. If the r_{iv0} of point D is assumed to be 0.88, i.e. D(0.88, $0.7744P_0$), the P_{ref} is determined as Eq. (11) for $\Delta V < 0$.

$$P_{ref} = P_{ref0} + \frac{-P_{ref0} + 1.21P_0}{0.1}(r_{iv0} - 1) \quad \Delta V > 0 \quad (10)$$

$$P_{ref} = P_{ref0} + \frac{P_{ref0} - 0.7744P_0}{0.12}(r_{iv0} - 1) \quad \Delta V < 0 \quad (11)$$

Note that point B or point D should be the first point of the intersection between P_{ref} and P_{load} characteristics. Additionally, these points should be stable ones, too.

The stability conditions of the operating points are discussed in Appendix A.1. For $\Delta V > 0$, point B is the first intersection between P_{ref} for any load that P_0 is less than P_{ref0} . Also, because the slope of the P_l characteristic at point B is greater than that of the P_{ref} characteristic, it is a stable operating point as explained in Appendix A.1.

Therefore, if islanding phenomenon occurs and ΔV is positive, the islanding will be detected. However, if islanding occurs and $\Delta V < 0$, the first stable intersection point between P_{ref} and P_{load} has a r_{iv0} that is greater than 0.88 and also is a stable point for some loads. This means that r_{iv0} reaches to this stable point and settle, i.e. the islanding is not detectable, and the NDZ of the method is not zero in islanding conditions.

To determine the NDZ of the method, the active load characteristic has been written as Eq. (12):

$$P_l = P_{l0} \left(\frac{V_p}{V_P} \right)^2 = P_{l0} r_{iv}^2 \quad (12)$$

As mentioned before, for $\Delta V < 0$, the proposed method can detect islanding phenomenon if the first stable intersection point between curves P_l and P_{ref} takes place at a point that r_{iv0} is less than 0.88. This is possible if the slope of P_{ref} is less than that of load curve at D(0.88, $0.7744P_0$). The slope of the load active power characteristic can be determined as follows:

$$\frac{d}{dr_{iv}}(P_0 r_{iv}^2) \Big|_{r_{iv}=0.88} = 2P_0 r_{iv} \Big|_{r_{iv}=0.88} = 1.76P_0 \quad (13)$$

In order to detect the islanding, the slope of the active power load at point that has $r_{iv}=0.88$ should be greater than that of P_{ref} .

$$1.76P_0 > \frac{P_{ref0} - 0.7744P_0}{0.12} \quad \text{or} \quad P_0 > 1.0146P_{ref0} \quad (14)$$

Then, for $P_0 \leq 1.0146P_{ref0}$, the islanding phenomenon is not detectable by the method. In other words, the NDZ of the proposed method is as follows:

$$0 \leq \frac{\Delta P}{P_{DG}} \leq 1.46\% \quad (15)$$

The P_{ref} that is shown in Eq. (11) cannot detect the islanding phenomenon for $P_0 < 1.0146P_{ref0}$. In order to reduce the NDZ to zero, the P_{ref} is determined as two linear functions of voltage for $P_0 < aP_{ref0}$ which a is a coefficient and should be greater than 1.0146. As previously mentioned, for load with $P_0 < 1.0146P_{ref0}$, P_{ref} as defined in Eq. (11) intersects the load curve at two points. The r_{iv0} of the first point is greater than 0.88 and is stable; the r_{iv0} of the second point is less than 0.88 and is an unstable operating point. Therefore, the PCC voltage decreases and reaches to the stable operating point ($r_{iv} > 0.88$) in islanding condition. If a is greater than 1.0146, the r_{iv0} of the intersection points of the load curve and P_{ref} are less than 0.88; the first point that has a greater r_{iv0} is stable operating point and the other one is unstable. Note that if a is a little greater than 1.0146, these two points are near together. Therefore, because of the transient behavior of islanding phenomenon, r_{iv0} may pass through the r_{iv0} of the unstable operating point. In other words, instability will occur in the PCC voltage. Simulation results show that if a is selected 1.05 or greater, the PCC voltage will be settled in the stable intersection point and then instability will not occur. Also for detecting the islanding phenomenon with high reliability, r_{iv0} of point D can be selected less than 0.88 (for instance 0.86, as it is specified in Fig. 2). In this case, P_{ref} for $\Delta V < 0$ and $P_0 > 1.05P_{ref0}$, which is defined in Eq. (11), will change to Eq. (16).

$$P_{ref} = P_{ref0} + \frac{P_{ref0} - 0.7396P_0}{0.14}(r_{iv0} - 1) \quad \Delta V < 0 \quad (16)$$

In order to reduce the NDZ to zero, P_{ref} is selected as piecewise linear function of voltage for $P_{ref0} < P_0 < 1.05P_{ref0}$; the first section of P_{ref} for loads that $P_{ref0} < P_0 < 1.05P_{ref0}$ is determined in such a way that passes through A(1, P_{ref0}). The slope of this line (i.e. m) at point A should be greater than that of the load curve at this point ($m > 2P_0$). In this situation the operating point of A is unstable in islanding condition as discussed in Appendix A.1. If m takes $2.1P_0$, the first

section of P_{ref} for $P_0 \leq 1.05P_{ref0}$ is determined as Eq. (17). Point E along this section of P_{ref} is determined in such a way that the first intersection point of the second section of P_{ref} with load active power curve passes through point like D'; the r_{iv0} of D' should be greater than or equal to 0.88. Point E is not unique and a lot of points can satisfy the above condition. In other words, the above condition can be satisfied if point E is on line L and $0.88 < r_{iv0} < 0.95$. For example, if the r_{iv0} of point D' is assumed to be 0.88 and E is selected with $r_{iv0} = 0.9$, the line that passes through points E and D' is formulated as Eq. (18).

$$P_{ref} = 2.1P_{ref0}(r_{iv0} - 1) + P_{ref0} \quad (17)$$

$$P_{ref} = \frac{0.79P_{ref0} - 0.7744P_0}{0.02}(r_{iv0} - 0.9) + 0.79P_{ref0} \quad (18)$$

where $0.9 < r_{iv0} \leq 1$ and $r_{iv0} < 0.9$ in Eqs. (17) and (18), respectively.

Note that if point D' (as shown in Fig. 3) is selected as D' (0.86, $0.7396P_0$), Eq. (18) changes to Eq. (19) for $r_{iv0} < 0.9$.

$$P_{ref} = \frac{0.79P_{ref0} - 0.7396P_0}{0.04}(r_{iv0} - 0.9) + 0.79P_{ref0} \quad (19)$$

In Fig. 2, line L which is drawn as Eq. (17) is the first section of P_{ref} for loads that their active powers are between P_{ref0} and $1.05P_{ref0}$. The second section of P_{ref} is line L₁ for curve C₁ which is drawn as Eq. (19).

Therefore, if P_{ref} is determined as Eq. (10) for $P_0 < P_{ref0}$, Eq. (16) for $P_0 > 1.05P_{ref0}$ and Eq. (17) and Eq. (19) for $P_{ref0} < P_0 < 1.05P_{ref0}$, the NDZ of the proposed method reduces to zero. In fact, the NDZ is only one point in which P_0 is exactly equal to P_{DG} . Note that, the slope of line L is only dependent on P_{ref0} for loads that satisfy the inequality $P_{ref0} < P_0 < 1.05P_{ref0}$. For example, in Fig. 2, lines L and L₂ are P_{ref} for load C₂ ($P_0 = 1.03P_{ref0} < 1.05P_{ref0}$) in which line L₂ passes through point E on line L and point D''(0.86, $0.7396P_0$) on curve C₂. Line L₃ is P_{ref} for load C₃ that passes through points A and D. Also, line L₄ is P_{ref} for load C₄ that passes through A and B.

In order to determine the equation of P_{ref} , first, the load active power in nominal voltage (P_0) should be calculated. If islanding phenomenon occurs, the post-islanding PCC voltage is different from the pre-islanding PCC voltage, depending on the difference between the DG active power generation ($P_{DG} = P_{ref0}$) and the local load active power ΔP . Equation (20) will result by substituting r_{iv0} in Eq. (7):

$$P_{DG} = P_{ref0} = r_{iv}^2 P_0 = r_{iv0}^2 P_0 \quad \text{or} \quad P_0 = \frac{P_{ref0}}{r_{iv0}^2} \quad (20)$$

In normal condition, if the PCC voltage does not vary, then $r_{iv} = 1$ and $P_0 = P_{ref0}$. However, if the voltage varies, then $r_{iv} \neq 1$ and P_0 and P_{DG} can be computed from Eq. (20).

In the proposed method, when the active power imbalance between DG and the local load in nominal voltage is high enough that the voltage deviation in post-islanding is less/more than U/O voltage relay settings, the islanding is detected by this relay. On the other hand, when the active power imbalance is low, application of the proposed method is highlighted. So, in the simulation results which are presented in the next section, some cases are considered in which the power exchange between the DG and the grid satisfies inequality (9). The flowchart of the proposed method is shown in Fig. 3.

Based on Eq. (1), at the nominal system frequency and voltage, the active power of the load is P_0 . When the system frequency is changed the load active power will be changed too, and in nominal voltage, it is equal to $P_0(1+k_p\Delta f)$. As mentioned earlier, the method has been formulated for $k_p=0$. The active power reference (P_{ref}) formula is a function of P_{ref0} , r_{iv0} and P_0 . When $k_p=0$, the value that is computed from Eq. (20) is P_0 . However in condition that $k_p \neq 0$, the computed value will be equal to $P_0(1+k_p\Delta f)$. Regardless of the value of k_p , the method uses the computed value of Eq. (20) for determining the active power reference of DG. In other words, the method formulation is irrelevant to the value of k_p . In general, if the voltage change is sensed, the active power reference will be switched from P_{ref0} to the new designed P_{ref} . Then, islanding phenomenon is detected if it takes place.

It is generally accepted that the parallel RLC load ($p=2$) which has a high quality factor and operates at resonance condition (unity power factor) is the worst case for islanding detection [9, 18, 20]. Therefore, in the simulation results, the DG is designed to operate at unity power factor and the local load is modeled as a constant RLC load.

4 Evaluation of the Proposed Method

In abnormal conditions, the voltage variation has a transient behavior. When the voltage deviation is sensed by the voltage measurement equipment and the relay, a little time is required until the voltage reaches to a new stable value. Various simulations in different conditions show that a delay of 100 msec is sufficient for this purpose in islanding conditions. Therefore, in simulation results, the PCC voltage will be considered as post-islanding PCC voltage and is denoted by V'_{p0} , 100msec after sensing of voltage changes. Also, the islanding voltage ratio in this situation ($r_{iv0}=V'_{p0}/V_0$) is named r_{iv01} . Using measured data (V'_{p0} , r_{iv01}), P_0 will be calculated from Eq. (20). Therefore, the active power reference of DG is determined as Eq. (10) for $P_0 < P_{ref0}$ ($\Delta V > 0$) and as Eq. (16) for $P_0 > 1.05P_{ref0}$ ($\Delta V < 0$). Also, it is determined as Eq. (17) and Eq. (19) for $P_0 \leq 1.05P_{ref0}$, dependent on r_{iv0} . In order to evaluate the proposed method, islanding and non-islanding conditions are simulated. In non-islanding phenomena, if the proposed

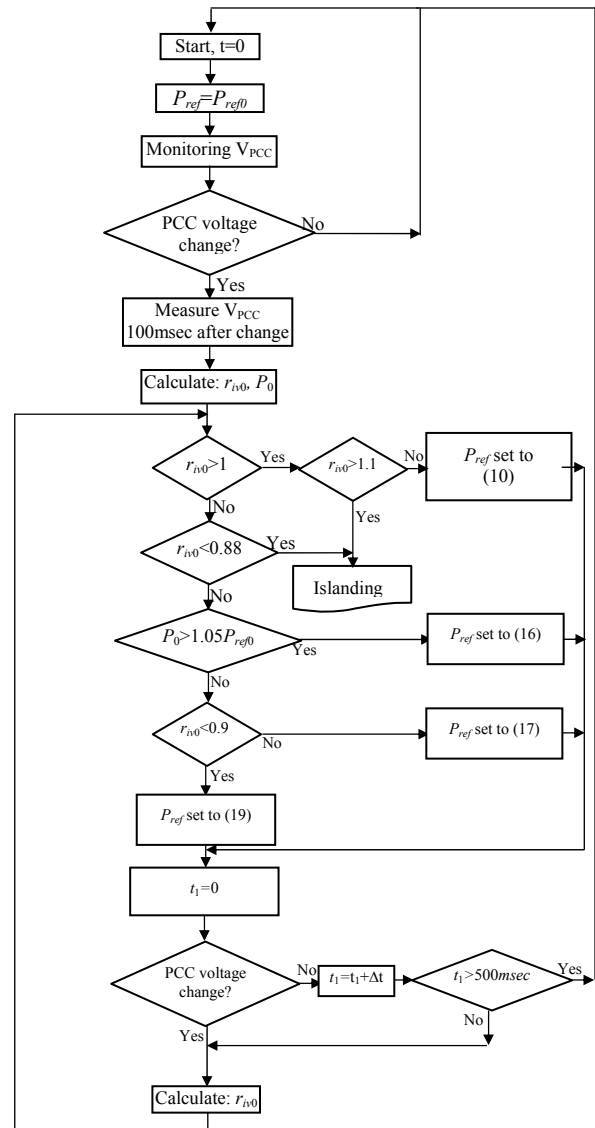


Fig. 3 The flowchart of the proposed islanding detection method.

method is used and the PCC voltage changes, the DG active power generation changes according to Eq. (10), Eq. (16), Eq. (17) and Eq. (19). In such cases, if the PCC voltage stays between the thresholds and remains stable for more than 500msec, the P_{ref} of DG can change into initial setting (P_{ref0}). The obtained results are presented and discussed in the following subsections.

4.1 Islanding Conditions

The proposed method is implemented on the study system shown in Fig. 1. The islanding phenomenon occurs at $t=3$ sec. The DG active power generation (P_{DG}) is considered to be 50 kW while the local load is assumed to have different values like 50 kW (fully matched), 49.5 kW and 50.5 kW (a little mismatch), 64.5 kW (lower bound of U/O voltage relay setting or

$\Delta P=0.2913P_{DG}$, 41.32kW (upper bound of U/O voltage relay setting or $\Delta P = 0.17355P_{DG}$) at nominal voltage. Note that k_p and k_Q are considered to be zero in the simulation results.

If P_{load} is assumed to be 50kW in nominal voltage (380 V) and islanding phenomenon occurs, then before voltage deviation and 100msec after that, the PCC voltage is equal to 379.949V and 378.217V, respectively. The r_{iv01} and P_0 can be computed and are equal to 0.997 and 50.25kW, respectively. The P_0 is less than $1.05P_{ref0}$ and then P_{ref} should be determined from Eq. (17) until $r_{iv0}\geq 0.9$, and from Eq. (19) when $r_{iv0}\leq 0.9$. For different load active powers, r_{iv01} , P_0 and P_{ref} are calculated and summarized in Table 2.

The variation of PCC voltage and DG active power using the proposed method for loads in Table 2 (50, 50.5, 64.5, 49.5 and 41.32 kW) are depicted in Fig. 4. If the proposed method is not used, the PCC voltage variations will not be enough to detect islanding (r_{iv01} in Table 2 less than 1.1 or greater than 0.88) for local loads that inequality (9) is satisfied. However, by using the proposed method, the voltage variations are enough for U/O voltage relay to detect the islanding phenomenon, which is shown in Fig. 4. Also, the DG active power variation is zero if the proposed method is not used. However, if the proposed method is used, the DG active power variation depends on the PCC voltage. The DG active power decreases or increases until the PCC voltage exceeds from U/O voltage relay thresholds.

It can be shown from Fig. 4 that using the proposed method, the post-islanding voltage variations are about 0.88/1.1 of the PCC nominal voltage for any loading conditions and the over voltage is not high. Note that all of the above simulation results show that islanding phenomenon is detected by the presented technique at the permitted time.

Fig. 5 shows the PCC voltage for different active power load voltage exponent (p) and $P_{load}=P_{ref0}=50$ kW with $Q_f=2.5$. It is shown that the islanding detection for $p=0$ and 1 is much simpler and faster than that of $p=2$. This is due to the fact that as the p for local load decreases, the PCC voltage deviation from nominal value increases more in islanding condition. In Fig. 6 the performance of the proposed method is shown for non-zero k_p ($k_p=3$) and it is compared with $k_p=0$. The resonance frequency of the local load (f_r) is considered to be 60.4 and simulations are done for $P_0=50$ kW and 49 kW ($P_0=49$ kW is the worst case of islanding detection for $k_p=3$ and $f_r=60.4$ Hz when the DG

Table 2 Determining P_{ref} for different loading cases.

Cases	P_{load} (kW)	V_P	V'_{r0}	r_{iv01}	P_0 (kW)	P_{ref} (kW)
1	50	379.9	379.0	0.9975	50.2	$58.4r_{iv0}-13$
2	50.5	379.8	377.4	0.9932	50.6	$50.3r_{iv0}-5.76$
3	64.5	376.4	336.0	0.8843	63.9	$19.33r_{iv0}+30$
4	49.5	380.0	380.8	1.0022	49.7	$102.3r_{iv0}-52.3$
5	41.3	381.8	414.8	1.0918	4.19	$7.54r_{iv0}+42.5$

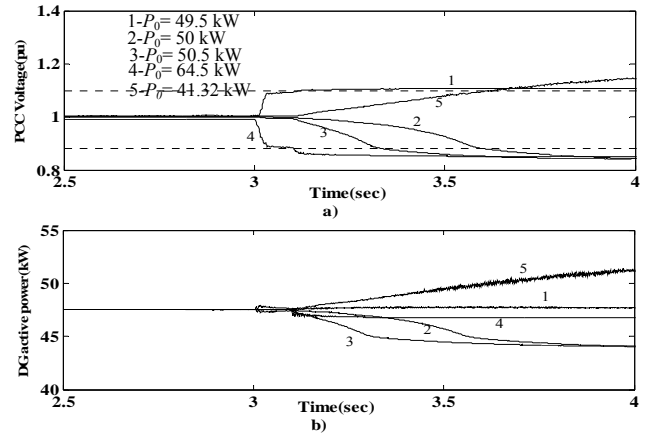


Fig. 4 Evaluation of the proposed method for different loadings: (a) PCC voltage and (b) DG active power.

generation is 50 kW). For different p and k_p , r_{iv01} and P_0 are calculated and summarized in Table 3; P_{ref} for these cases will be calculated as explained in section 3. P_0 in the cases 1 to 6 are less than $1.05 P_{ref0}$ and greater than P_{ref0} , therefore, P_{ref} is piecewise linear function of voltage for these cases which is determined from Eq. (17) as $105r_{iv0}-55$ for $r_{iv0}\geq 0.9$ and from Eq. (19) for $r_{iv0}\leq 0.9$ that are shown in Table 3.

For case 5 of Table 3, load active power is 49 kW in nominal voltage and frequency, but 100msec after islanding; its calculated value is 50.3kW. This value is equal to P_0 for case 3. This can be seen in curves 2 and 3 of Fig. 6 that islanding is detected almost in the same time for these cases after islanding. On the other hand, because of the load frequency dependency, the case 5 in Table 3 is also the worst case for islanding detection, as case 3.

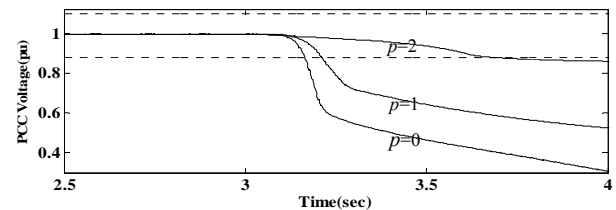


Fig. 5 PCC voltage in islanding condition for $p = 0, 1$ and 2 , $k_p = 0$ and $P_{load} = 50$ kW

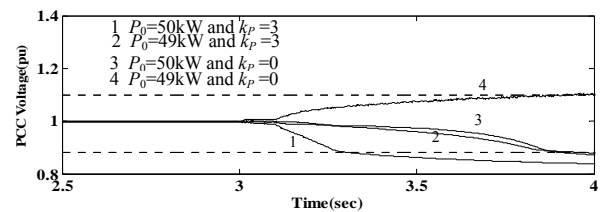


Fig. 6 PCC voltage in islanding condition for $p = 2$, $k_p = 0, 3$ and $P_0 = 50, 49$ kW

Table 3 Determining P_{ref} for different p and k_p .

Cases	f_r (Hz)	Q_f	P_{load} (kW)	V_P	V'_{P0}	r_{iv01}	P_0 (kW)	P_{ref0} (kW)
1 ($p=0, k_p=0$)	60	2.5	50	379.63	377.32	0.993	50.7	$50.057r_{iv0}-5.551$
2 ($p=1, k_p=0$)	60	2.5	50	379.63	378.33	0.996	50.4	$55.604r_{iv0}-10.544$
3 ($p=2, k_p=0$)	60	2.5	50	379.63	378.75	0.997	50.3	$57.453r_{iv0}-12.208$
4 ($p=2, k_p=3$)	60.4	2.5	50	378.54	375.21	0.987	51.2	$40.812r_{iv0}-2.769$
5 ($p=2, k_p=3$)	60.4	2.5	49	378.16	378.85	0.997	50.3	$59.302r_{iv0}-13.8718$
6 ($p=2, k_p=0$)	60.4	2.5	50	378.54	378.05	0.995	50.5	$53.755r_{iv0}-8.88$
7 ($p=2, k_p=0$)	60.4	2.5	49	378.16	381.64	1.0043	49.6	$100.16r_{iv0}-50.16$

Table 4 Determining P_{ref} for non-islanding conditions.

Cases	Conditions	V_P	V'_{P0}	r_{iv01}	P_0 (kW)	P_{ref} (kW)
1	5% increase in system voltage	379.613	397.765	1.0467	45.6	$52.2r_{iv0}-2.16$
2	10% increase in system voltage	379.613	416.731	1.097	41.6	$3.36r_{iv0}+46.6$
3	5% decrease in system voltage	379.613	361.86	0.952	55.1	$65.8r_{iv0}-15.83$
4	10% decrease in system voltage	379.613	343.119	0.9029	61.3	$33.1r_{iv0}+16.9$
5	400 μ F capacitor switch on at t=3sec	379.613	400.381	1.0536	45	$45r_{iv0}+5.03$
6	400 μ F capacitor switch off at t=4sec	398.891	379.613	0.999	50.1	$61.1r_{iv0}-15.5$
7	50kW load switched on at t=3sec	379.613	368.927	0.971	53	$76.9r_{iv0}-26.9$
8	50kW load switched off at t=4sec	368.927	379.458	0.9986	50.1	$51.9r_{iv0}-7.2$

4.2 Non-islanding Conditions

In this section the performance of the proposed method has been tested on the system under study in non-islanding phenomena. The load is a 50 kW RLC load. The phenomena like system voltage variation, capacitor bank switching and variation of local load have been considered. Results of the examining of the phenomenon are presented in Fig. 7. The Fig. 7(a) shows the PCC voltage variation when the system voltage decreases and increases 10% and 5% at t=3sec as a step function, whether the proposed method is used or not. The voltage deviation is sensed, then P_{ref} switches to the determined P_{ref} at t=3.1sec, as mentioned above. Fig. 7(b) shows the curve of the PCC voltage variation for capacitor switching; at t=3sec a 400 μ F capacitor bank (21.78 kVAr) has been paralleled to the local load and at t=4sec it is switched off. At t=3sec the voltage variation has been sensed, therefore P_{ref} changes from P_{ref0} to the determined P_{ref} at t=3.1sec. The PCC voltage deviation is not enough for islanding detection and also it is constant; after 500 msec, P_{ref} jumps to P_{ref0} . At t=3sec, because of the capacitor bank switching off, another voltage deviation is sensed; after 100msec, P_{ref} is switched to a new one. The simulation is done in condition whether the proposed method is used or not. Also, Fig. 7(c) illustrates the results when another 50 kW load with $Q_f=1.8$ is switched on in parallel with the existing load at t=3sec and switched off at t=4sec. Note that, P_{ref} changes like capacitor bank switching case, at t=3.1sec, t=3.5sec and t=4.1sec. In Table 4 r_{iv01} , V'_{P0} and P_{ref} are calculated and summarized for non-islanding conditions.

The simulation results in non-islanding conditions show that in all cases (decreasing or increasing of system voltage, switching the capacitor bank and load), only operating point has been changed and the condition has not been detected as islanding. It can be seen from

Fig. 7 that there is a small difference on the PCC voltage variation in the condition that the proposed method is used or not. However, because the DG active power reference depends on the PCC voltage, the impact of the proposed method on the DG active power generation is significant. So, if the PCC voltage changes, DG active power generation changes too. If necessary, the DG active power generation can be returned to the previous setting.

4.3 Effects of Load Quality Factor on the Performance of the Proposed Method

Quality factor (Q_f) is an important parameter in the islanding detection behavior techniques. Therefore, this has been mentioned in different references. For instance, it is emphasized that for loads with Q_f less than 1.8, the islanding should be detected in less than two seconds [10, 18, 20-22]. In fact, islanding detection is difficult for the load with high Q_f [10]. Also based on IEEE Std. 929, the islanding should be detected in case of the loads with Q_f less than 2.5 [18]. In addition, the applied method should be capable to detect the islanding for loads with Q_f greater than 0.5, as stated in [23]. In this paper, in order to investigate the performance of the proposed method, different load quality factors have been considered. Islanding phenomenon is simulated for 50 kW load active power and different Q_f like 0.5, 1.5, 2.5 and 4. In these conditions, r_{iv01} , P_0 , V_P , V'_{P0} and P_{ref} are calculated and presented in Table 5. For cases of Table 5, P_{ref} has been calculated from Eq. (19) until $r_{iv0} \geq 0.9$ and from Eq. (21) when $r_{iv0} < 0.9$. Fig. 8 shows the simulation results. It can be seen that for all considered quality factors, islanding phenomenon is detected at the permitted time.

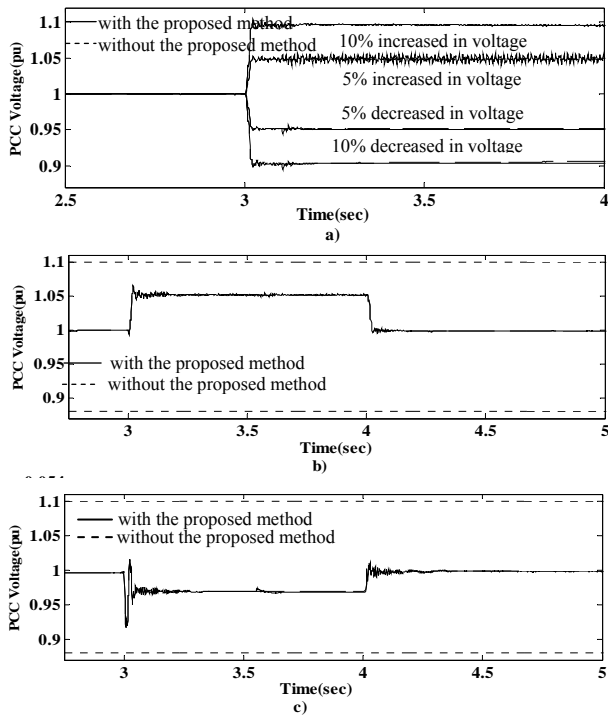


Fig. 7 Evaluation of the proposed method for non-islanding conditions: (a) system voltage change, (b) capacitor switching and (c) load switching.

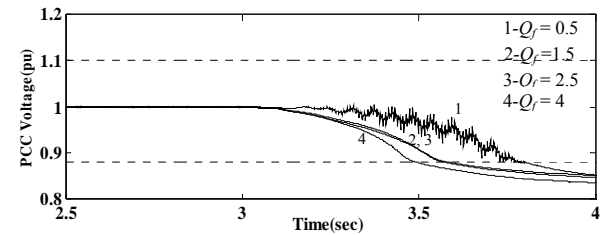


Fig. 8 Effect of load quality factor on the performance of the proposed method.

Table 5 Determining P_{ref} for different Q_f when P_{load} is equal to 50kW.

Cases	Q_f	V_F	V'_{F0}	r_{i01}	P_0 (kW)	P_{ref} (kW)
1	0.5	379.908	379.388	0.998	50.16	$60r_{i0} - 14.5$
2	1.5	379.579	378.782	0.997	50.3	$57r_{i0} - 11.8$
3	2.5	379.96	378.799	0.9968	50.3	$57r_{i0} - 11.8$
4	4	380.358	378.54	0.9962	50.4	$55.8r_{i0} - 10.7$

4.4. Comparing with the Presented Technique in [8]

In this subsection the proposed method is compared with the presented technique in [8]. As mentioned in Table I of [8], the NDZ of the presented method is not zero. Two cases are considered for simulations; first, the active power reference of DG is demonstrated by a linear function of the PCC voltage as described in reference [8] ($P_{ref}=0.1r_{i0}-0.05$). Then, another case is considered where P_{ref} is determined by the proposed method in section 3. Simulation results show that the NDZ of the presented method in [8] is approximately

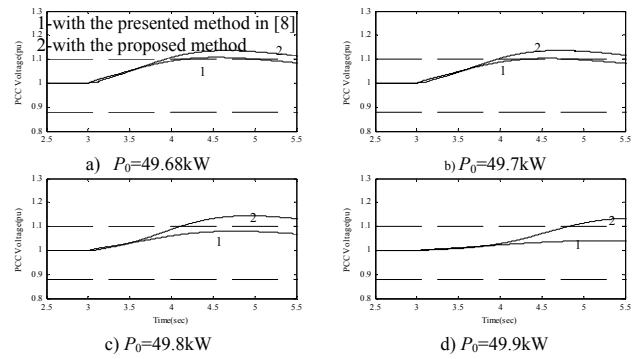


Fig. 9 Comparing the proposed method with the presented method in [8].

between 49.68 kW and 49.95 kW. The active power generation of DG is assumed to be 50 kW, while local load is considered in the NDZ of [8] with $Q_f=1.8$ and islanding simulation will be done for two mentioned cases. Fig. 9 illustrates the results when islanding phenomenon occurs at $t=3$ sec. It is evident that the presented method in [8] is failed; meanwhile, islanding is detected by the proposed method in all loading conditions.

5 Conclusion

In this paper a new islanding detection technique for inverter based DG is presented. The method is based on the change in DG active power reference and is an adaptive one. If the PCC voltage does not change, P_{ref} is equal to P_{ref0} . If the PCC voltage changes, the P_{ref} will change, too. The P_{ref} is determined adaptively by computing load active power and post-islanding PCC voltage. The DG active power reference is determined as a linear function of PCC voltage. When islanding phenomenon occurs, the proposed method reaches the PCC voltage to the upper or lower thresholds of the U/O voltage relay. The proposed method does not have any NDZ. If the PCC voltage is changed due to non-islanding phenomena, the effect of the proposed method in voltage variation will be almost zero. Also, the proposed technique is reliable, i.e. it detects islanding when it is and it does not detect when it is not. The effectiveness of the proposed algorithm is demonstrated by simulation results. In addition, it is shown that for all cases, islanding phenomenon is detected at the permitted time.

Appendix

A.1 Stability Conditions of the Operating Point

If the slope of the load characteristic (P_l) at the operating point is greater than that of the load active power reference (P_{ref}), this point will be a stable operating point. Also, if the slope of P_l at the operating point is smaller than that of the P_{ref} , this point is unstable. More details can be found in Fig. A.1.

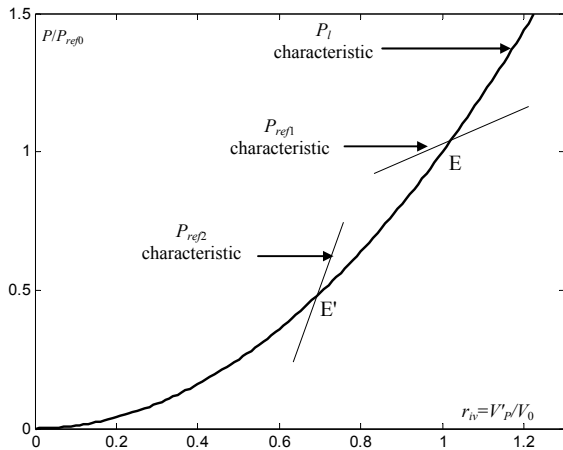


Fig. A.1 Load active power and P_{ref} characteristics for showing the stability condition of the operating points.

Suppose P_{ref1} is the P_{ref} characteristic. The slope of the load characteristic is greater than that of the P_{ref} characteristic at point E, then, this point is a stable operating point. For showing the stability of point E, suppose this point to be the operation point and a small positive deviation takes place in voltage. Therefore, in this case $P_l > P_{ref}$, P_l is decreasing to reduce the difference between P_l and P_{ref} . In order to decrease P_l , voltage should decrease, too. It means that for positive voltage deviation, operating point will come back to point E.

The same procedure will be applied if the voltage deviation is negative. Hence, it can be concluded that point E in Fig. A.1 is stable. On the other hand, if P_{ref2} is the P_{ref} characteristic at point E', the slope of the load characteristic is smaller than that of the P_{ref} characteristic. Therefore, this point is an unstable operating point. For showing the instability of point E', suppose this point to be the operating point and a small positive deviation take place in voltage. Therefore, in this case $P_l < P_{ref}$, P_l is increasing to reduce the difference between P_l and P_{ref} . In order to increase the P_l , voltage should increase too. It means that operating point will have more deviation from E'. The same procedure will be applied if the voltage deviation is negative. Thus, point E' is an unstable operating point.

A.2 System Parameters

The parameters of the grid system, line and transformer are presented in Tables A-1 and A-2.

Table A-1 Parameters of the grid system.

Nominal voltage	380 V
System frequency	60 Hz
Internal resistance	0.06 Ohm
Internal inductance	0.9 mH

Table A-2 Line and transformer characteristics.

380V line reactance	0.2734Ω
380V line resistance	0.05937 Ω
Transformer short circuit impedance	4%

References

- [1] IEEE Standard for interconnecting distributed resources with electric power systems, 1547-2003, Jul. 2003.
- [2] Salman S. K., Kin D. J. and Weller G., "New loss of main detection algorithm for embedded generation using rate of change of voltage and changes in power factors", *Developments in Power System Protection, IEEE Conference*, Amsterdam, pp. 82-85, Apr. 2001.
- [3] Refern M. A., Usta O. and Fielding G., "Protection against loss of utility grid supply for a dispersed storage and generation unit", *IEEE Trans. on Power Del.*, Vol. 8, No. 3, pp. 948-954, Jul. 1993.
- [4] Ropp M., Aaker K., Haigh J. and Sabhah N., "Using power line carrier communications to prevent islanding", *Proc. 28th IEEE Photovoltaic Specialist Conference*, Anchorage, Ak, pp. 1675-1678, Sep. 2000.
- [5] Xu W., Zhang G., Li C., Wang W., Wang G. and Kliber J., "A power line signaling based technique for anti-islanding protection of distributed generators-part I: scheme and analysis", *IEEE Trans. on Power Del.*, Vol. 22, No. 3, pp. 1758-1766, Jul. 2007.
- [6] Wang W., Kliber J., Zhang G., Xu W., Howell B. and Palladino T., "A power line signaling based scheme for anti-islanding protection of distributed generators -part II: field test results", *IEEE Trans. on Power Del.*, Vol. 22, No. 3, pp. 1767-1772, Jul. 2007.
- [7] Mahat P., Chen Z. and Bak-Jensen B., "A hybrid islanding detection technique using average rate of voltage change and real power shift", *IEEE Trans. on Power Del.*, Vol. 24, No. 2, pp. 764-771, Jul. 2009.
- [8] Zeineldin H. H. and Kirtley J. L., "A simple technique for islanding detection with negligible non-detection zones", *IEEE Trans. on Power Del.*, Vol. 24, No. 2, pp. 779-786, Apr. 2009.
- [9] Bower W. and Ropp M., "Evaluation of islanding detection methods for photovoltaic utility interactive power systems", *Int. Energy Agency Implementing Agreement on Photovoltaic stems*, Tech. Rep. IEA PVPS T5-09, Mar. 2002.
- [10] Hernandez-Gonzalez G. and Iravani R., "Current injection for active islanding detection of electronically-interfaced distributed resources", *IEEE Trans. on Power Del.*, Vol. 21, No. 3, pp. 1698-1705, Jul. 2006.
- [11] Ma T.T., "Novel voltage stability constrained positive feedback anti-islanding algorithm for the inverter-based distributed generator systems", *IET Renew. Power Gener.*, Vol. 4, No. 2, pp. 176-185, Mar. 2010.

- [12] Liu F., Kang Y., Zhang Y., Duan S. and Lin X., "Improved SMS islanding detection method for grid-connected converters", *IET Renew. Power Gener.*, Vol. 4, No. 1, pp. 36-42, 2010.
- [13] Smith G. A., Onions P. A. and Infield D. G., "Predicting islanding operation of grid connected PV inverters", *Proc. IEE Electric Power Applications*, Vol. 147, No. 1, pp. 1-6, Jan. 2000.
- [14] Kunte R. S. and Wenzhong G., "Comparison and review of islanding detection techniques for distributed energy resources", *40th North American Power Symposium (NAPS '08)*, Calgary, AB, pp. 1-8, Sep. 2008.
- [15] Velasco D., Trujillo C. L., Garsera G. and Figueres E., "Review of anti-islanding techniques in distributed generators", *Renewable and Sustainable Energy Reviews*, Vol. 14, No. 6, pp. 1608-1618, Aug. 2010.
- [16] Wang X., Freitas W., Xu W. and Dinavahi V., "Impact of DG interface controls on the sandia frequency shift anti-islanding method", *IEEE Trans. on Energy Convers.*, Vol. 22, No. 3, pp. 792-794, Sep. 2007.
- [17] Kundur P., *Power System Stability and Control*, McGraw Hill Inc., Newyork, 1994.
- [18] IEEE Recommended practice for utility interface of photovoltaic systems, *IEEE Standard 929-2000*.
- [19] Tsili M. and Papathanassiou S., "A review of grid code technical requirements for wind farms," *IET Renewable Power Generation*, Vol. 3, No. 3, pp. 308-332, Sep. 2009.
- [20] UL 1741 Standard for Static inverter and charge controllers for use in photovoltaic systems, *UL 1741 Standard*, 2001.
- [21] UL 1741 Standard for Converters and controllers for use in independent power systems, *UL 1741 Standard*, 2001.
- [22] Schauder C. and Mehta H., "Vector analysis and control of advanced static VAR compensators", *Proc. Inst. Elect. Eng.*, Vol. 15, No. 3, pp. 299-306, Jul. 1993.
- [23] Woyte A., Belmans R. and Nijs J., "Testing the islanding protection function of photovoltaic inverters", *IEEE Trans. on Energy Convers.*, Vol. 18, No. 1, pp. 157-162, Mar. 2003.



Ebadollah Kamyab was born in Larestan, Iran. He received the B.Sc. and M.Sc. both from Ferdowsi University of Mashhad, Mashhad, Iran. He served as a high voltage Electrical Engineer at the Khorasan Regional Electric Company, Mashhad, Iran from 1992. Since 2007 he has been studying toward his Ph.D. degree at Ferdowsi University of Mashhad, Mashhad, Iran. His research interests are Distributed Generation, Power System Protection and Transformer.



Javad Sadeh was born in Mashhad, Iran in 1968. He received the B.Sc. and M.Sc. with honour both in Electrical Engineering from Ferdowsi University of Mashhad, Mashhad, Iran in 1990 and 1994, respectively and obtained his Ph.D. in Electrical Engineering from Sharif University of Technology, Tehran, Iran with the collaboration of the electrical engineering laboratory of the Institut National Polytechnique de Grenoble (INPG), France in 2001. He is currently an associate professor in the Department of Electrical Engineering at Ferdowsi University of Mashhad, Mashhad, Iran. His research interests are Power System Protection, Dynamics and Operation.